Nationaal Onderzoeksprogramma
Broeikasgassen
Veenweiden

Chapter 9 NOBV year report 2022

Temporal variation in nitrous oxide emission from grassland on drained peat soil

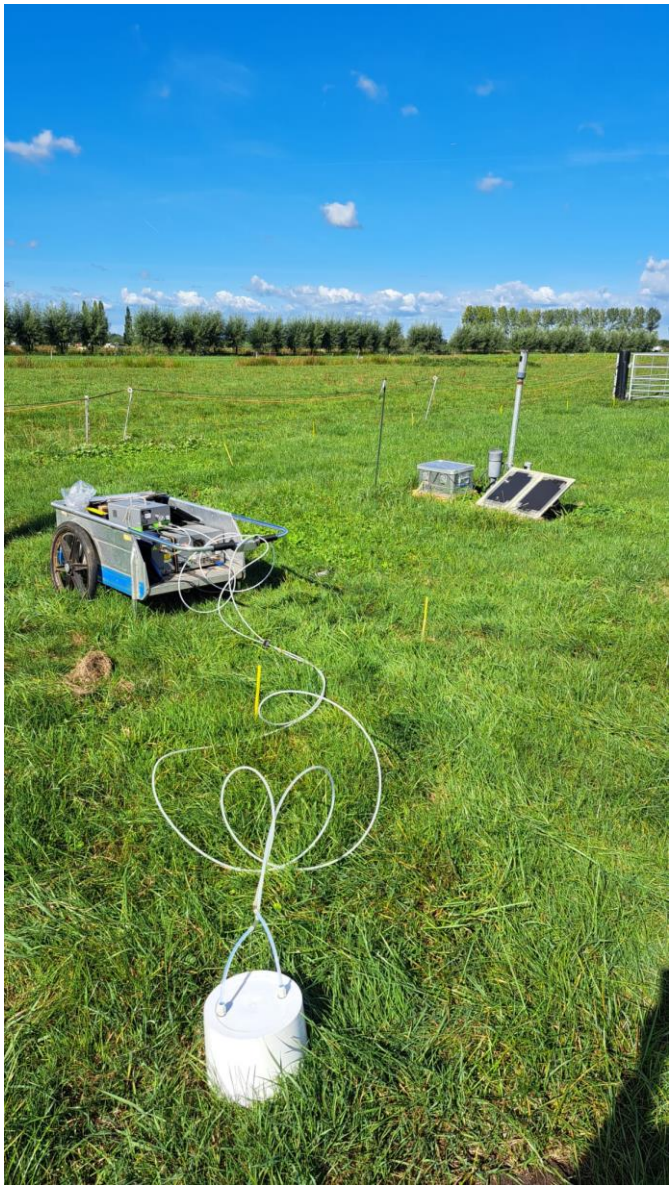

Temporal variation in nitrous oxide emission from grassland on drained peat soil

Authors
Gerard Velthof[1]
Jordy van 't Hull[1]
Ralf Aben[3]
Christian Fritz[3]
Sarah Faye Harpenslager[4]

Affiliation
[1]Wageningen Environmental Research, Wageningen
[3]Radboud Universiteit, Nijmegen
[4]B-WARE Research Centre, Nijmegen

Abstract

The microbial processes nitrification and denitrification are the major sources of the greenhouse gas nitrous oxide (N_2O) emitted from soils. Conditions for N_2O emission are favourable in managed drained peat soils due to the combination of shallow groundwater levels and high contents of mineral nitrogen (N) and available carbon (C). Here, we assessed the temporal variation in N_2O fluxes from grassland on drained peat soil, on diurnal to monthly scale using automated chambers during winter, and on weekly to inter-annual scale using weekly measurements with static chambers during four years. Automated chamber measurements during winter showed relatively low emissions (on average < 120 µg N m^{-2} h^{-1}), but with clear diurnal variation, with highest fluxes occurring during night-time. However, these diurnal variations as well as correlations of N_2O fluxes with CO_2 fluxes and photosynthetically-active radiation almost completely disappeared when only days without atmospheric stratification were assessed. This indicates that chambers can greatly overestimate background N_2O fluxes during non-turbulent atmospheres via disturbance of the N_2O gradient in the soil-vegetation system by the chamber, which has so far only been shown for CO_2. As atmospheric stratification may also influence N_2O production (e.g., by affecting moisture content), data from longer timeseries are needed to verify the dominant role of a methodological bias versus any true biogeochemical effect of atmospheric stratification on N_2O emissions. Large annual variations in N_2O emission were shown over a 4-year period (10.5–33.5 kg N ha^{-1} yr^{-1}), caused by interannual differences in precipitation during the growing season. High N_2O emission peaks occurred directly after N application during wet conditions. Periods with elevated N_2O emission were captured during less than 25% of the measurements over four years, but comprised 76% of the total N_2O emission. Quantifying mitigation measures to reduce N_2O emission from drained peat soils requires a combination of measurement techniques, i.e., static chamber measurements at discrete intervals to compare mitigation options in a statistically-sound experimental design, combined with automated chambers and eddy co-variance for insight in factors controlling N_2O emission, gap-filling and extrapolation to a larger temporal and spatial scale. As a large part of the annual N_2O emission is produced during relatively short events after N application and precipitation events, measurement strategies should focus on accurate quantification of these N_2O peaks.

1 Introduction

Soils are a major source of the greenhouse nitrous oxide (N_2O). On a global scale, managed and natural soils contribute to 56-70% of the total anthropogenic N_2O emission (Butterbach-Bahl et al., 2013). In soils, N_2O is mainly produced during the microbial processes of nitrification and denitrification (Firestone, 1982; Wrage-Mönnig et al., 2018). Soil type and conditions, weather conditions, and nitrogen (N) fertilisation have a strong effect on N_2O production in soils (Butterbach-Bahl et al., 2013). Rapid changes in soil contents of mineral N (e.g., by application of N fertilisers and manure), available carbon (e.g., by application of crop residues and manure), oxygen (e.g., rainfall, groundwater fluctuations, and biological oxygen consumption in the soil) and temperature can result in strong fluctuations in N_2O emission. The highest N_2O production can be found in fertilised soils during relatively wet soil conditions, and especially in soils rich in organic matter (e.g., grassland soils, peat soils or soils to which organic matter containing products are applied). Temperature also affects the production of N_2O in soils, as nitrification and denitrification rates increase with temperature. However, in some studies the proportion of N_2O in the total N loss (N_2O / (N_2 + N_2O)) decreases with temperature, so that the net effect of temperature on N_2O emission is affected by two counterbalancing factors (Firestone, 1982; Maag and Vinther, 1996).

Peat soils are drained for agricultural use. Conditions for N_2O emission are more favourable in managed drained peat soils than in managed mineral soils. Quantification of N_2O emission from grasslands on mineral soils and peat soils with similar nutrient management (fertilisation and grazing), showed that N_2O emission from peat soils were about a factor 2 to 4 higher than those from mineral soils (Velthof et al., 1996a). The N_2O emission from unfertilised and mown grassland was about a factor five higher in peat soils than in mineral soils. Emissions of N_2O from peat soils amounted up to 13% of total European N_2O emissions in 2011, while peat soils represented only 7% of the EU land area (Leppelt et al., 2014). The denitrification capacity in peat soils is higher than in mineral soils, because the higher organic matter content in peat soils provides an energy source for denitrifying bacteria (Munch and Velthof, 2007). In addition, a high biological oxygen demand resulting from high organic matter contents and shallow groundwater tables decrease oxygen content and create favourable conditions for N_2O production(Dickopp et al., 2018) .

Drained peat soils are also a large source of CO_2 emission (Frolking et al., 2011). Options to decrease CO_2 emission from peat soils include raising the water table and using water infiltration systems to impede decomposition of organic matter (Boonman et al., 2022). Changes in water management in peat areas also affect the risk of N_2O emissions (Lin et al., 2022; Taft et al., 2018). On the one hand, limiting organic matter decomposition by rewetting peat soils decreases N mineralisation and the resulting N_2O emission. On the other hand, the oxygen content associated with rewetting may stimulate N_2O production through denitrification. Production of N_2O increases with decreasing oxygen concentrations in the soil, but at very low oxygen conditions, i.e., anaerobic conditions, N_2O is reduced to N_2 (Weier et al., 1993). The balance between these factors is understudied thus far and better insight in the effect of water and nutrient management on N_2O emission from drained peat soils is required to make substantiated management and policy decisions.

Temporal variation of N_2O fluxes is high, which is caused by changes in mineral N contents, water contents, and temperature throughout the year (Anthony & Silver, 2021; Velthof et al., 1996a). Fluxes of N_2O peak just after application of mineral fertiliser or manure and during wet conditions. Rainfall and strong changes in groundwater level, especially if sufficient mineral N is available, can therefore result in high N_2O fluxes. Some studies showed diurnal variations in N_2O emission, which are mainly caused by diurnal variations in temperature (e.g. Maljanen et al., 2002). Spatial

variation of N_2O fluxes is also high, which is due to heterogeneity in soil factors controlling N_2O production and emission, and their interactions (Velthof et al., 1996b)

Different methods for quantification of N_2O emission are used in scientific literature, each with pros and cons. Static chamber methods are widely used in field and incubation studies for quantification of N_2O emission (de Klein et al., 2020). These methods can be used for comparison between different treatments (e.g., different fertilisation) in a statistical field set-up with replication. However, N_2O measurements with static chambers are often discontinuous in time (sometimes only once per week), because many chambers have to be measured within an experimental set-up. Calculation of total N_2O emission over the experimental period is generally based on linear interpolation of the measured fluxes or on gap filling methods using other parameters, e.g. rainfall and temperature (Dorich et al., 2019; Dorich et al., 2020). Automatic chambers directly connected to a gas analyser have the advantage that measurements can be carried out more frequently than with manual chamber methods (Smith and Dobbie, 2001). However, these systems are much more expensive than static chambers and they are generally only used in experiments with a limited number of treatments. Micro-meteorological methods, such as the eddy co-variance method, have the advantage that they measure continuously and integrate fluxes over a larger area (Kroon et al., 2010). These methods require a large area with a uniform treatment and can therefore not be used in experiments with replicated treatments.

In this paper, we analysed and compared the temporal variation in N_2O fluxes from grassland on drained peat soil based on detailed continuous measurements of N_2O fluxes with automatic chambers during winter and inter-annual variations based on weekly measurements with static chambers. We hypothesised that diurnal variation in N_2O emission only occurs during periods with relatively low emissions, when temperature is the main factor causing temporal variations in N_2O fluxes. Moreover, we hypothesised that N_2O emission peaks induced by N fertilisation and rainfall events contribute for the majority of the total annual N_2O emission, as opposed to background emissions that occur throughout the entire measurement period. The results will be used to discuss strategies of measurements of N_2O emission in time and options for gap filling in order to obtain the most accurate estimates of N_2O emission.

2 Materials and methods

2.1 Study area

Measurements with automatic chambers and static chambers were carried out on a managed grassland field on a peat soil in Zegveld in the Netherlands (Parcel 16 of the experimental dairy farm in Zegveld, located in the Western part of the Netherlands: 52°26′N, 4°48′E). The grasslands had a *Lolium perenne* sward and had been intensively managed for more than 25 years. The grassland had been intensively managed with fertilisation with mineral fertiliser and cattle slurry and by grazing. The plots on which static chamber measurements were carried out, were fertilised with calcium ammonium nitrate (CAN) fertiliser. The N application rates were 210, 250, 250 and 210 kg N per ha per year, for 2019, 2020, 2021, and 2022, respectively. The N application was split in 4 to 5 dressings. Soil properties are shown in Table 1. The average water level in the ditches surrounding the experimental plots was 55 cm below the soil surface, and the plot was not connected to a water infiltration system. The automatic chamber measurements were carried during the period October 2022 – January 2023. The static chamber measurements were carried out for four years: 2019 – 2022.

The monthly precipitation and monthly average temperature were derived from stations of Royal Netherlands Meteorological Institute (KNMI) in Zegveld and De Bilt (Table 1 and Figure 5). The total amount of rainfall was highest in 2019 (964 mm) and lowest in 2021 (805 mm). The highest emissions were expected in the period March – 1 September, because this is the period in which N fertiliser is applied to grassland. March 2019 was relatively wet and March 2022 was extremely dry. April and July were relatively dry in all years. May 2021, June 2019, June 2022 were relatively wet.

Table 1. Soil properties of Parcel 16 of Zegveld experimental farm.

Soil layer, cm	**Total N***	**Total P***	**Total C****	**pH-H_2O**
	g/kg	g/kg	g/kg	
0-30	15.2	2.2	169.7	5.7
30-60	21.7	1.0	304.3	5.3
60-90	23.8	0.6	373.0	5.3

*Soil digestion using H_2SO_4-H_2O_2-Se

**LECO-CHN analyzer

Table 2: Monthly precipitation (measured in Zegveld) and average temperature (measured in de Bilt)..Source: KNMI.

Month	**Precipitation, mm**					**Temperature, °C**			
	2019	**2020**	**2021**	**2022**		**2019**	**2020**	**2021**	**2022**
Jan	63	52	84	47		3.5	6.2	3.4	5.3
Feb	64	148	47	116		6.1	7.2	4.3	6.8
Mar	103	64	38	7		8.0	6.8	6.4	7.3
Apr	33	10	47	58		10.9	11.1	6.7	9.3
May	68	21	123	53		11.7	13.1	11.2	14.0
Jun	116	77	58	104		18.1	17.5	18.2	17.1
Jul	42	82	41	22		18.8	17.0	18.0	18.6

Aug	63	66	81	47		18.4	20.4	16.9	20.0
Sep	98	71	15	129		14.5	15.2	15.9	14.6
Oct	120	125	133	47		11.6	11.3	11.6	13.1
Nov	115	48	79	100		6.4	8.9	7.4	8.6
Dec	78	104	61	84		5.8	5.5	5.4	3.9
Total	964	866	805	813					

2.2 Automated transparent chamber measurements

Fluxes of N_2O between the soil-vegetation system and atmosphere were calculated from N_2O concentration changes measured from October 2022 until January 2023 using automated transparent chambers (eosAC-LT; Eosense) with a total height of 41.2 cm and volume of 72 L. These chambers consist of a transparent base (height: 15 cm; SA: 0.21 m2) and dome-shaped lid that is controlled by a linear actuator. The plot was equipped with three chambers connected to a multiplexer (eosMX, Eosense) that routed gas to a MIRA Ultra mid-IR $N_2O/CO/H_2O$ analyser (Aeris Technologies). The analyser measured at 1-sec intervals and was connected in a parallel configuration to the outlet tube of an infrared CO_2/H_2O gas analyser (LI-850, LI-COR). Recirculation of gas in the chamber system was achieved using the LI-850's built-in pump (0.75 L/min) and PTFE tubing (10 m length, one way; 3.2 mm ID). Each chamber was measured once during each cycle using a 2.5-min closure time and 15-sec flushing period before and after chamber closure. Every half hour a CR1000x datalogger initiated a new measurement cycle by sending a command to the multiplexer. Permanent serrated soil collars (15 cm deep) were installed in 3 adjacent rows upon which chambers were rotated every two weeks to minimise effects of continuous chamber presence on the soil-vegetation system. These collars offset the original chamber height by 0–1.5 cm and are considered by adjusting the total gas volume used in the flux calculation. The eosAC-LT chambers are equipped with a headspace temperature sensor and a low-flow fan to achieve a well-mixed headspace (Christiansen et al., 2015; Rochette and Hutchinson, 2005) .

Gas concentration data of automated chambers were removed in case the analyser's cell pressure or temperature were outside the calibrated operating range, resulting in 0.22% data loss. N_2O concentrations during chamber closures were also visually inspected to identify abnormalities. This resulted in the removal of 1881 out of 10398 individual N_2O chamber measurements, which was fully attributed to chamber 1 that suffered from a malfunctioning multiplexer valve for 51 days. Hence, of the final flux dataset, chamber 1 contributed 18% of fluxes, whereas chamber 2 and 3 each contributed 41% of fluxes.

Fluxes of N_2O were calculated using the gasfluxes package (Fuss, 2020) that includes an approach to select automatically between the linear or non-linear flux estimate of each chamber measurement, based on the N_2O analyser's uncertainty and the flux sise (Hüppi et al., 2018). This approach allows for non-linear estimates without forcing non-linear estimates on linear concentration changes, thereby decreasing the flux estimates' uncertainty. We used this automated selection method to estimate fluxes under turbulent atmospheric conditions, as determined by ambient CO_2 concentrations <= 420 ppm. Under stable atmospheric conditions—that are usually restricted to night-time—a build-up of gases near the surface occurs. Closure of the automated chamber, equipped with a low-mixing fan, then leads to a disturbance of the established CO_2 gradient in the soil-vegetation system, causing a flush of CO_2 (and most likely other emitted gases that have accumulated) that can lead to great overestimation of fluxes (Juszczak et al., 2012; Koskinen et al., 2014; Figure 1 in the Appendix). Following recommendations in Koskinen et al. (2014), we attempted to limit the effect of pulse emissions

during stable atmospheric conditions by using (robust) linear regression and delaying the starting time of the regression. Based on mixing times (including analyser response time) observed in the lab during injections of different amounts CO_2 in a chamber on an impermeable base (Figure 2 in the Appendix), we postponed the starting time of the regression with 60 seconds for moderately stable atmospheres (i.e. CO_2 concentration at start of chamber closure > 420 ppm and CO_2 concentration at end of chamber closure <= 900 ppm) and 90 seconds for highly stable atmospheres (i.e. CO_2 concentration at start of chamber closure > 420 ppm and CO_2 concentration at end of chamber closure > 900 ppm). Note, however, that these mixing times still need to be determined for N_2O. As they may deviate from those of CO_2, so may the time needed to postpone the start of the regression for the various degrees of atmospheric turbulence. For now, we assumed that these thresholds for CO_2 also provide a good proxy for the regressions to determine N_2O fluxes.

From 8517 quality-controlled chamber measurements, 45% were evaluated according to a turbulent atmosphere, 54% to a moderately-stable atmosphere and 1% to a highly stable atmosphere (Figure 3 in the Appendix). The high precision of the N_2O measurement combined with our chamber setup resulted in a minimum detectable flux (Christiansen et al., 2015; Maier et al., 2022; Nickerson, 2016) of 9.2 µg N m^{-2} h^{-1}. This enabled us to detect very small fluxes despite short (2.5 min) chamber closures and resulted in only 0.8% of chamber measurements having flux estimates that were statistically indistinguishable from zero at the $p < 0.01$ level.

Environmental variables
Soil moisture and temperature were measured at 10-cm intervals from 5–115 cm depth, using Drill & Drop capacitance probes (Sentek, Australia) that were installed in the vicinity of each automated flux chamber. Data measured at 1-min intervals was logged as 30-min averages.

Air temperature, humidity, and pressure (30-min logging interval) as well as wind speed and direction (1-min logging interval) were measured at 2-m height using a MaxiMet GMX500 (Gill instruments Limited, UK). Precipitation was measured using a ARG314 tipping bucket rain gauge (Environmental Measurements Limited, UK). Photosynthetically-active radiation (PAR) was measured at 2-m height (1-min logging interval) using a SKR 1840D (Skye Instruments, UK).

2.3 Static chamber measurements

Static chamber measurements of N_2O emission were carried out in three replicates (three plots) in the period March 2019 – January 2023. At the beginning of the experiment, a polyvinylchloride (PVC) collar of 20 cm diameter and 10 cm height was installed permanently into the soil to a depth of 5 cm at the centre of each plot to provide a base for the measurements (Hutchinson and Mosier, 1981). These collars were only removed during harvesting and N application for a short period of time and were afterwards installed on exactly the same place. During N_2O measurements, gas-tight chambers were placed on top of these collars to create a closed system of 4.7 L chamber volume. To allow gas sampling during measurements, the chambers were equipped with a rubber septum and vent tubes on the top. N_2O concentration analyses were performed with a PICARRO G2508 cavity ring-down spectroscopy gas analyzer (PICARRO, USA). Static chamber measurements were performed weekly during the growing season (March - September), but frequency was temporarily increased to two samplings during the week after N application. Outside the growing season, the frequency decreased to fortnightly samplings on average.

After the chambers were placed on top of the collar, air was sampled using the PICAtRRO analyzer after 10 minutes. The N_2O fluxes were calculated using the following equation:

$$Flux = \frac{(C_t - C_0)V}{\Delta t * V_m * m * \beta * A} \quad (1)$$

With the flux in µg N_2O-N $hr^{-1}m^{-2}$. C_t and C_0 the N_2O concentration in the headspace at the measurement time and closing time of the headspace, respectively, in parts per million (ppm; µl L^{-1}); Δt the time between closure and measurement in h; V the volume of the chamber in L; V_m the molar volume of a gas at standard temperature and pressure (V_m = 22.4 L mol^{-1}); m the molar mass of N_2O: 44 g mol^{-1}; A the area of the chamber in m^2; and β a conversion factor to convert between N_2O and N_2O-N (β = 28/44). Flux rates were expressed as the mean (n = 3) with the standard deviation of the replicated plots. The accumulated annual N_2O-N emission was calculated by linear interpolation between the measured daily fluxes. Soil temperature and soil moisture was collected at a depth of 10 cm, using a TDR soil probe (TRIMO-PICO 32, IMKO Micromodultechnik GmbH, Germany) at an hourly time interval.

Porewater was biweekly collected in plots where static chamber measurements were conducted between April and October in both 2021 and 2022. Ceramic porewater cups were installed at 20-25 cm depth. Porewater was collected by attaching a 60 mL syringe and manually creating a vacuum. Before sample collection, syringes and ceramic cups were flushed with 5-10 mL of porewater. Collected porewater was transferred to plastic containers and frozen on site. Samples were collected every couple of weeks and transported to the laboratory in Nijmegen for analysis. Concentrations of nitrate and ammonium were measured colourimetrically on an auto-analyser (Bran+Luebbe auto-analyser III system) using salicylate reagent and hydrazine sulphate, respectively. Acidified samples (0.1 ml 65% HNO_3) were analysed for Ca^{2+}, Mg^{2+}, Fe^{2+}, total-P and total-S using inductively coupled spectrometry (ICP-OES ARCOS, Spectro Analytical Instruments, Germany).

3 Results and discussion

3.1 Automated transparent chamber measurements

During the study period, we found a mean emission of 47, 101 and 120 µg N m^{-2} h^{-1} for automated chamber 1, 2 and 3, respectively (consider missing data for chamber 1, see Methods). These emissions are in the range previously observed in lab and field studies of peat soils at similar soil water content conditions (e.g. Anthony and Silver, 2021; Säurich et al., 2019) and match with the IPCC emission factors (94 µg N m^{-2} h^{-1}, 95%CI [56, 126]) for N_2O emissions from grassland on deep-drained, nutrient-rich organic soil (IPCC, 2014). Note, however, that the latter represents mean annual emissions, while we only have data for the autumn–winter period that largely doesn't include the effects of hot moments caused by fertilisation and large changes in soil water content (Anthony and Silver, 2021). Our N_2O emission monitoring detected a short period of elevated emission in the second half of November 2022. Peak emission reached 750 µg N m^{-2} h^{-1}, coinciding with elevated soil moisture levels and soil temperature falling below 6°C.

Mean normalised N_2O fluxes show a general trend for all 3 chambers of relatively low fluxes during daytime—with minimum values around solar noon—and high fluxes during night-time (Figure 1a). This coincides with a similar, but much clearer diurnal pattern for the CO_2 fluxes (Figure 1b), where low fluxes during daytime mostly represent net CO_2 uptake (Figure 2). Accordingly, significant nonlinear (quadratic) relationships (all $P < 1 * 10^{-7}$) were found between the mean normalised CO_2 flux and the mean normalised N_2O flux for the different chambers (Figure 3a). For mean hourly normalised CO_2 fluxes, a very strong relationship (quadratic regression [QR]; all $P < 1 * 10^{-15}$) was found with mean hourly photosynthetically-active radiation (PAR) for all chambers (Figure 3b). This relationship with mean hourly PAR was also found for the mean hourly normalised N_2O flux (QR; all $P < 1 * 10^{-7}$), albeit clearly weaker (Figure 3c). The relationship between individual N_2O fluxes and PAR at the time of chamber closure was significant for all chambers (QR; P = 0.0006, 0.0003 and 0.02 for chamber 1, 2 and 3, respectively), but rather weak (Figure 3d).

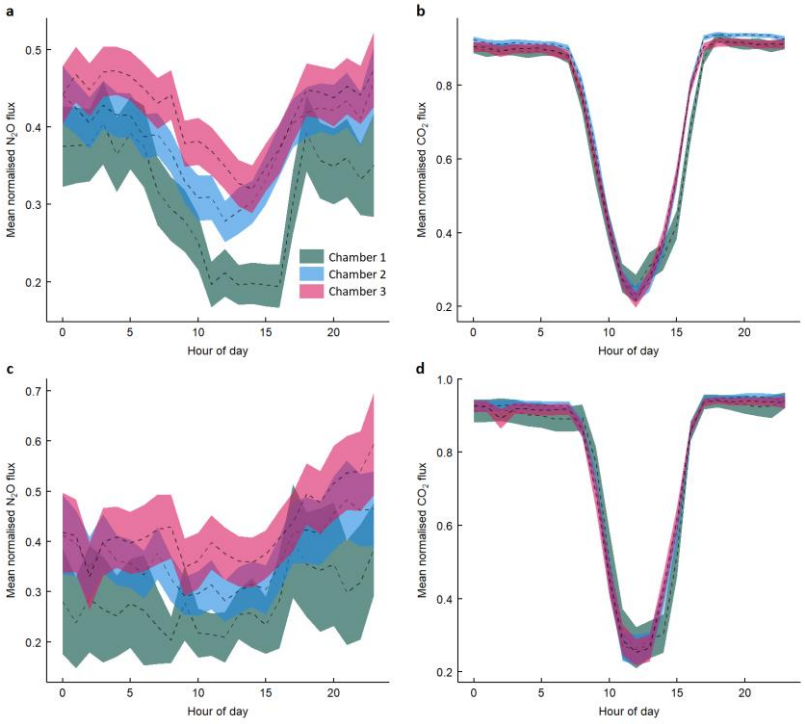

Figure 1. Diurnal variation of mean normalised N_2O (a) and CO_2 (b) fluxes for the full study period and full dataset, and diurnal variation of mean normalised N_2O (c) and CO_2 (d) fluxes for the full study period filtered by CO_2 concentrations <= 420 ppm at the start of chamber closure to largely exclude measurements in stable atmosphere. Fluxes were normalised per chamber for each day via min–max scaling (0–1). All normalised fluxes calculated for the period of interest were subsequently binned by hour of day. Dashed lines represent the mean hourly normalised values for each chamber. Shaded areas represent the standard error about the mean normalised hourly values.

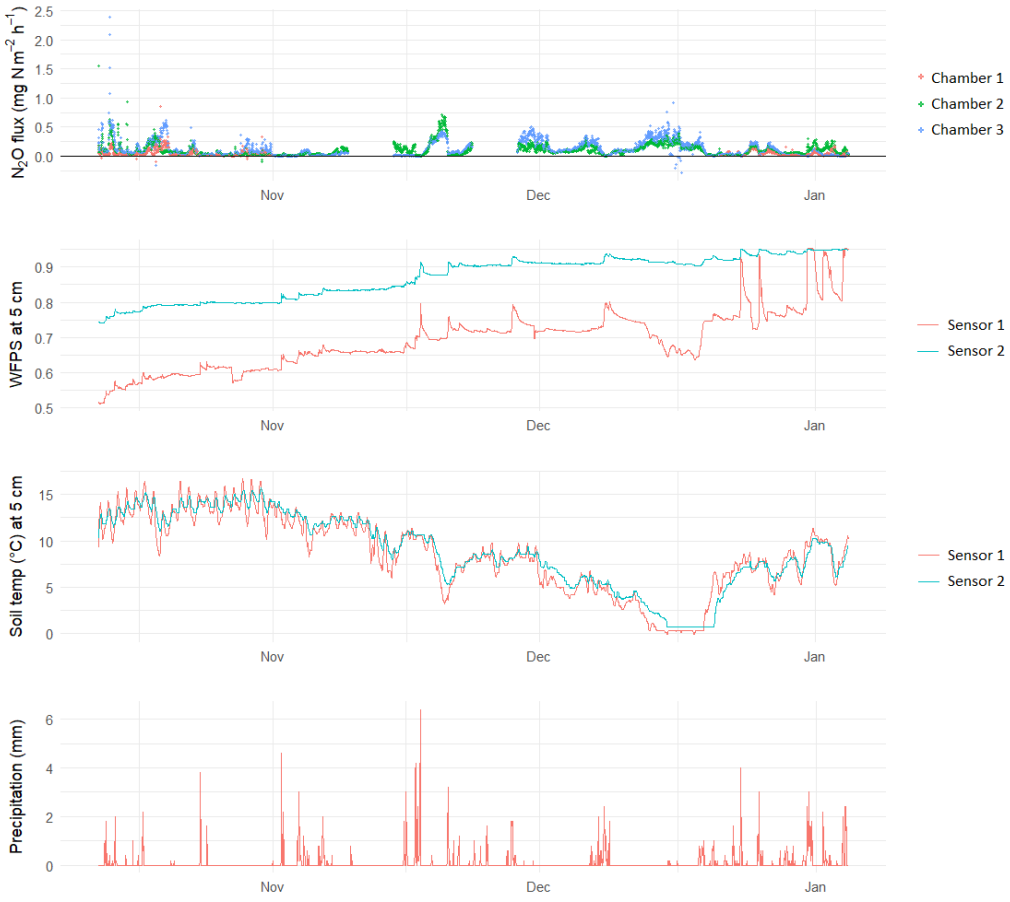

Figure 2. Timeseries of N_2O fluxes, water-filled pore space at 5 cm depth (estimated from soil moisture data via calibration with tensiometers), soil temperature at 5 cm, and precipitation during the study period.

Our observations contrast those of Keane et al. (2018a), who found higher normalised N_2O fluxes during daytime in the energy crop oilseed rape (*Brassica napus*), a negative relationship between the mean hourly normalised CO_2 flux and mean hourly normalised N_2O flux, and a positive relationship between (mean hourly) PAR and (normalised) N_2O fluxes. They hypothesize that most N_2O was produced by denitrification, driven by organic C produced during photosynthesis. The latter may not play an important role in our system, as availability of easily degradable organic C in our peat soils is much higher than in the system studied by Keane et al. (2018a). On the other hand, readily degradable carbon is responsible for fast microbial responses to changes in soil biogeochemistry. Perhaps in carbon-rich grasslands (on peat soils), concentrations of NH_4^+ and NO_3^-—produced via mineralisation and nitrification— are lowered during the day due to plant uptake, thereby limiting N_2O fluxes. However, this seems unlikely as these grasslands are intensively managed and rich in nitrogen. Even outside of the growing season, inorganic-N is typically high due to mineralisation of N-rich organic matter and limited uptake by plants.

An alternative explanation is that the common stable atmospheric conditions during the study period may have resulted in an overestimation of night-time N_2O fluxes, despite our correction efforts. The removal of measurements with CO_2 concentrations > 420 ppm at the start of the measurement—used as a proxy for atmospheric stratification—results in almost the complete removal of the diurnal pattern observed for normalised N_2O fluxes in the full dataset (Figures a, c), without an obvious effect for that of CO_2 (Figures b, d). Also, relationships of (normalised) N_2O fluxes with normalised CO_2 fluxes and PAR (as shown in Figure 3) were severely weakened or became nonsignificant when only using the subset of data filtered by estimated atmospheric turbulence (Figure 4 in the Appendix).

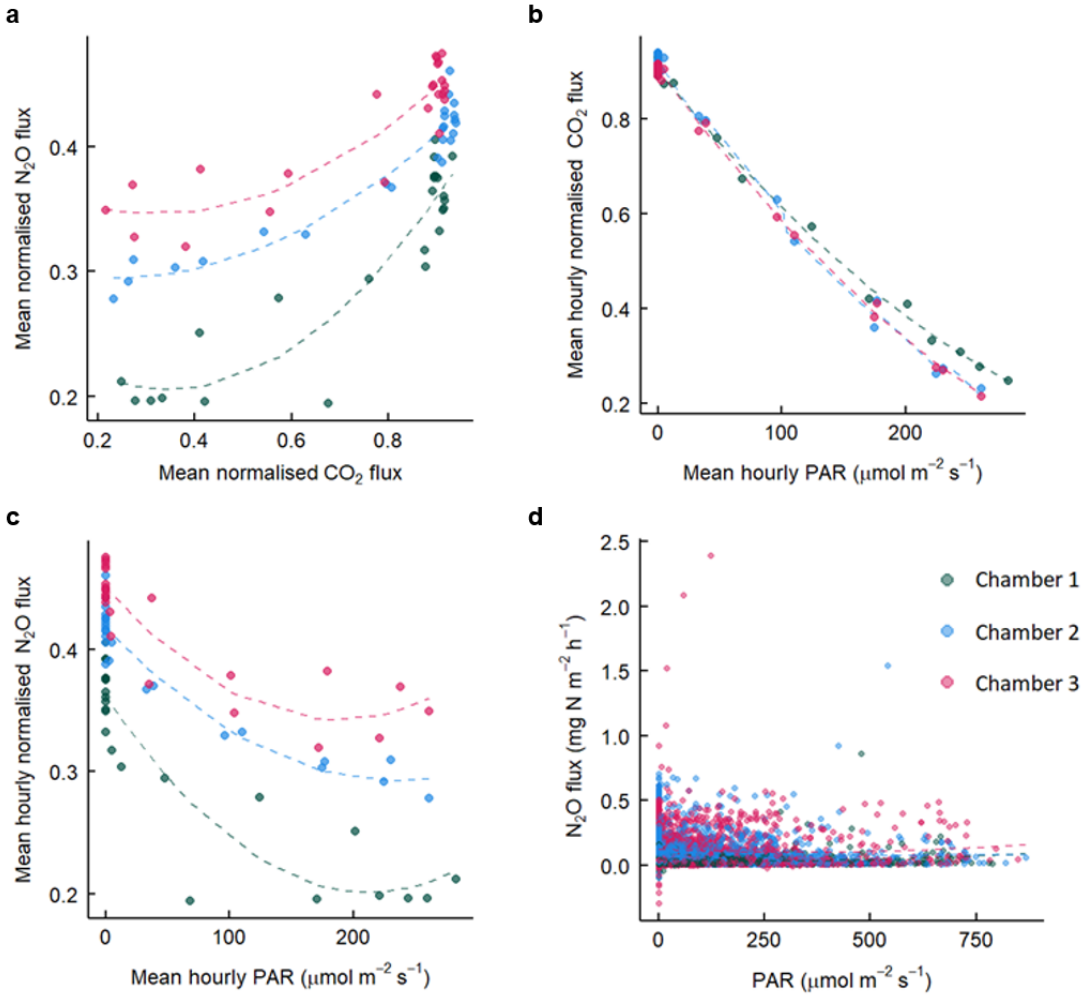

Figure 3. Plots of the normalised N_2O flux against the mean normalised CO_2 flux (a), mean hourly photosynthetically-active radiation (PAR) against the mean hourly normalised CO_2 flux (b), mean hourly PAR against the mean hourly normalised N_2O flux (c), and (d) PAR against the N_2O flux. Normalisation of data was achieved per chamber and day by min–max scaling (0–1) and subsequent binning by hour of day.

The difference in diurnal patterns that we observed between the full dataset and subset filtered by atmospheric stratification (Figure 1) is comparable to that observed by Brændholt et al. (2017) for soil CO_2 fluxes in a beech forest. Even if the fluxes that we estimated are accurately corrected for the initial flush and related mixing time of stored CO_2 and N_2O (see Methods & Figures 1 and 2 the Appendix), one must wonder if these estimates are truly unbiased. Accumulation of CO_2 and N_2O on the soil surface can develop during periods with a low-turbulent atmosphere (usually restricted to night-time), reduces the concentration gradient between soil and atmosphere and thereby the

diffusive flux, which in turn results in subsoil accumulation of these gases (Brændholt et al., 2017). Chamber closure and related mixing of CO_2- and N_2O-rich gas on the soil surface with less rich air in the chamber headspace causes a sudden drop in CO_2 and N_2O concentrations just above the soil surface and thereby increases the soil–atmosphere concentration gradient for these gases (Brændholt et al., 2017; Görres et al., 2016). This increases the diffusive flux, resulting in flux overestimates as this is not happening outside of chambers. Any consequent drop in subsoil CO_2 and N_2O storage inside of chambers is likely quickly restored in between the 30-min measurement cycles via diffusion from the surrounding soil, thereby likely causing structural overestimation of fluxes while atmospheric stabilisation lasts. This problem has been described in the literature for CO_2 fluxes (Brændholt et al., 2017; Görres et al., 2016; Juszczak et al., 2012; Koskinen et al., 2014; Lai et al., 2012; Schneider et al., 2009), but as far as we know, we are the first to show this for N_2O. As the bias introduced by low-turbulence conditions is difficult, if not impossible, to correct for (Brændholt et al., 2017; Lai et al., 2012; Schneider et al., 2009), some authors have suggested to exclude fluxes measured during low-turbulent conditions (e.g. Juszczak et al., 2012). This seems a straightforward solution for CO_2 fluxes estimated from long-term, automated chambers, as small gaps created by the removal of low-turbulent nights can be reliably filled using Random Forest or other advanced gap-filling techniques ((Aben et al., 2023) Zhu et al., 2023). However, the typical erratic N_2O fluxes and their complex underlying processes are much more difficult to predict. This severely complicates gap-filling (Dorich et al., 2020) and may require a large set of predictor variables (Goodrich et al., 2021). These predictors should include reliable estimates of soil nitrogen concentration and nitrogen uptake potential by plants.

Simple exploratory analyses did not show a clear effect of water-filled pore space and soil temperature for both the full and reduced dataset (Figures 4b, d), even though water-filled pore space as well as temperature can be important predictors for N_2O emission (Anthony and Silver, 2021; Keane et al. (2018a). Using eddy covariance technique (Wecking et al., 2020) found the highest N_2O emission at 70% waterfilled pore space (WFPS). As our measurements were performed in autumn and winter, we may already have missed key changes in soil water content that are known to cause peak emissions (Anthony and Silver, 2021). In spring and summer small rain events may be sufficient to spark N_2O emission upon moisture increase in the topsoil (Wecking et al. 2020). Any remaining effects of water-filled pore space and soil temperature may be masked by interactions with other variables. We did observe a clear relationship between windspeed and N_2O fluxes (quadratic fit, all $P < 1 * 10^{-15}$), with lower windspeeds generally corresponding to higher emissions (Figure 4a). Even for the reduced dataset, this relationship is still present, albeit clearly weakened (Figure 4c), with P values for quadratic fits being $< 1 * 10^{-8}$, $< 1 * 10^{-10}$ and $< 1 * 10^{-16}$ for data from chamber 1, 2 and 3, respectively. Windspeed can be a proxy for atmospheric stabilisation and its related bias on chamber-based flux estimates. The significant relationship of estimated N_2O fluxes and windspeed in the reduced dataset may thus indicate that our filtering procedure to exclude stable atmosphere measurements wasn't stringent enough. Consequently, the trend of increasing normalised hourly N_2O fluxes that we see between late afternoon and midnight in the filtered dataset (Figure 1c) may still be a result of atmospheric stabilisation starting to develop. Since our analyser has a small offset in the CO_2 concentration, our slightly conservative threshold CO_2 concentration of 420 ppm used to filter fluxes may already mean an accumulation of 20–30 ppm above the true atmospheric concentration. In addition, one must consider the magnitude of data loss caused by our filtering procedure and its effects on being able to detect diurnal patterns. Only full days (i.e. >= 23 hours of flux measurements) were included in our analyses for diurnal variation (Figure 1) to avoid biases. As a result, the full dataset contained 32, 71 and 71 days of data for chamber 1, 2, and 3, respectively, (Figures 1a, b), while the reduced dataset only contained 8, 21 and 21 days for chamber 1, 2, and 3, in the reduced dataset respectively (Figures 1c, d). Also, although a methodological bias during nights with atmospheric stratification seems the most likely reason of the observed diurnal pattern of normalised N_2O fluxes (and disappearance of it after filtering for turbulent atmospheres; Figure 1), we should be careful to not disregard any true diurnal variation that may be related to stable atmosphere conditions. For example, oxygen concentrations in the soil may decrease during

atmospheric stratification and the high relative humidity that is typical of stable atmospheres may affect the water content of the topsoil. Both changes in oxygen and soil water content can affect the biogeochemical processes that cause N_2O emission. In support of this, we see that the diurnal pattern of normalised water-filled pore space in the top 5 cm of the soil—like that of the normalised N_2O flux—largely disappears after filtering for turbulent atmospheres (Figure 5 in the Appendix). Hence, a reanalysis of diurnal patterns when a longer timeseries is available will give us more insight into the potential effects of methodological biases versus mechanistic processes that may drive diurnal variation. Reanalysis of data will also include alternative filtering methods, such as filtering based on friction velocity or mean vertical wind speed as a more direct measure of atmospheric turbulence (Goodrich et al., 2021; Lai et al., 2012; Pastorello et al., 2020; Schneider et al., 2009).

Future monitoring and reporting will focus on more on the frequency of high-emission events and environmental factors associated with high emission (Figure 2).

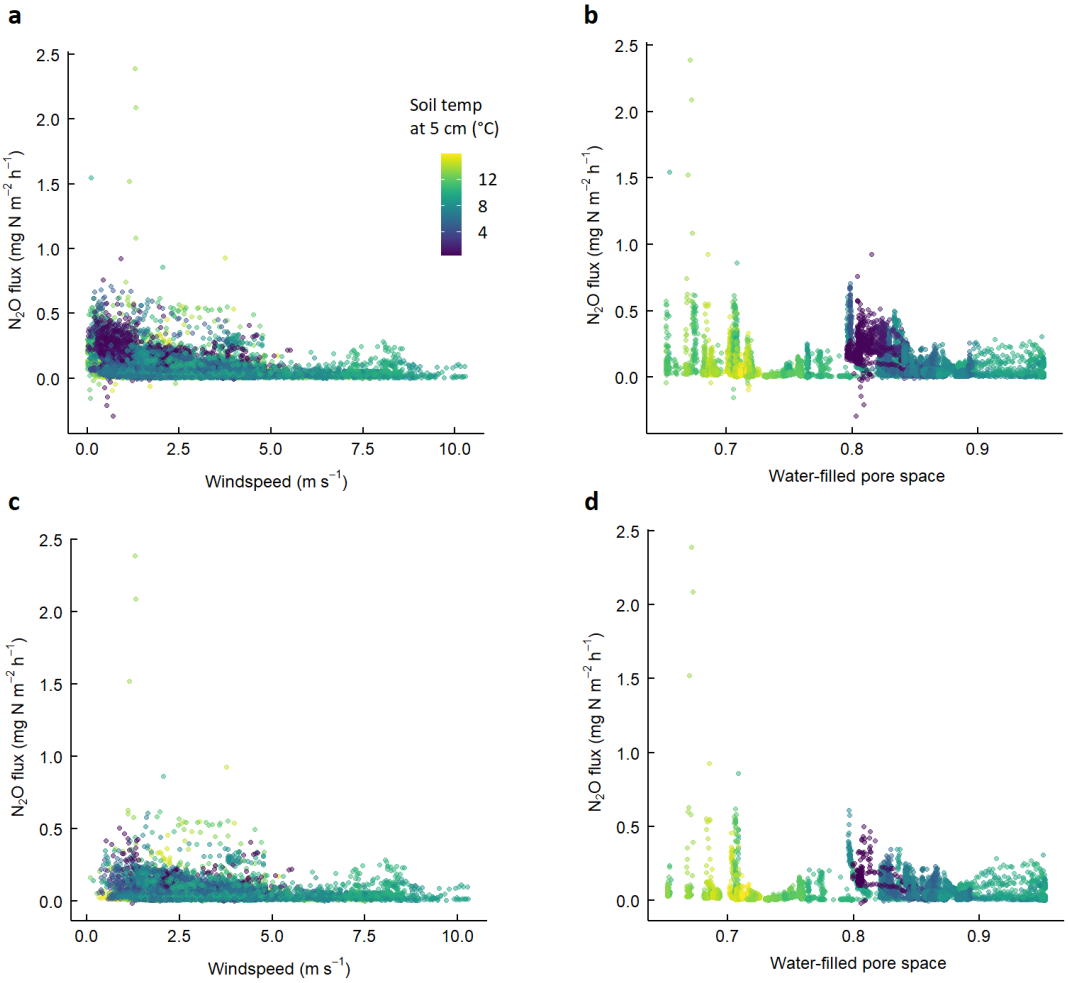

Figure 4. Water-filled pore space at 5 cm depth (estimated from soil moisture data via calibration with tensiometers; mean of 2 sensors) against N_2O fluxes (a) and windspeed against N_2O fluxes (b). The same is shown in c and d for a subset of data filtered by CO_2 concentrations <= 420 ppm at the start of chamber closure to largely exclude measurements in stable atmosphere. Dot colorisation denotes the soil temperature at 5 cm (mean of 2 sensors).

3.2 Static chamber measurements

Throughout the measuring period (2019 – 2022) there were several peaks in N_2O fluxes per year, with fluxes up to 2.5 mg N m^{-2} hr^{-1} (Figure 5). These peaks are generally related to the application of N fertiliser during relatively wet conditions (high precipitation and high groundwater levels; Figure 5). Of the measured fluxes, 75% was smaller than 0.2 mg N m^{-2} hr^{-1} (Figure 6). The annual N_2O emission was 17.8 kg N ha^{-1} yr^{-1} on average and ranged from 10.5 kg N ha^{-1} yr^{-1} in 2019 and 2022 to 33.5 kg N ha^{-1} yr^{-1} in 2021 (Table 3). Peak emissions, here defined as N_2O emissions ≥ 0.2 mg N m^{-2} hr^{-1}, occurred at 25% of measurement moments (Figure 6) and contributed to the total annual emission for an average of 76%, ranging from 66% in 2019 to 88% in 2021. Clearly, the peaks in N_2O emission strongly determined the total annual N_2O emission from fertilised grassland on drained peat soil. Similar results were found in a study of Anthony and Silver (2021) in California USA, in which hot moments of N_2O emissions from a corn field on a drained peat soil represented 1.1 ± 0.2% of measurements, but contributed to 45 ± 1% of mean annual N_2O fluxes. Hot moments were defined in this study as individual flux measurements that were more than 4 standard deviations from the yearly mean.

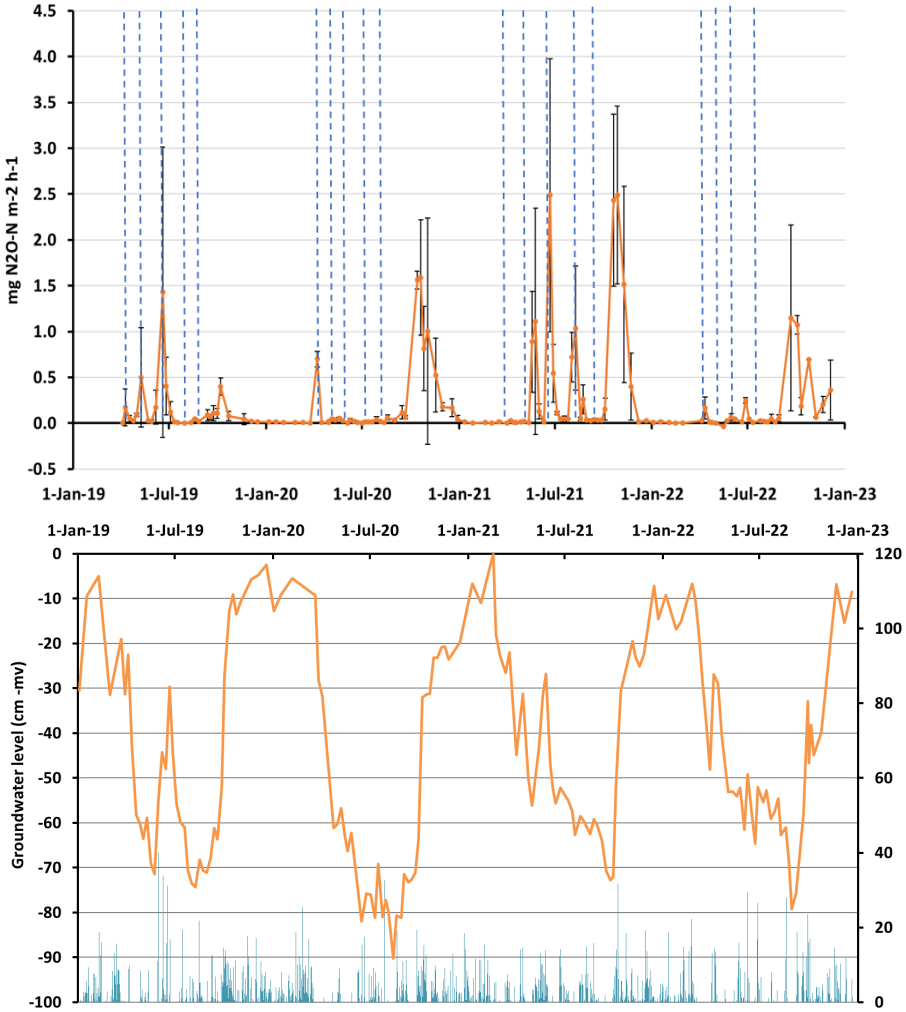

Figure 5. Upper figure: Fluxes of N_2O from fertilised grassland on drained peat soil derived with static chamber measurements in the period March 2019 to January 2023. The vertical blue lines indicate the times of application CAN fertiliser. The error bars show the standard deviation of the three replicates. Lower figure: precipitation and groundwater level in the period March 2019 to January 2023.

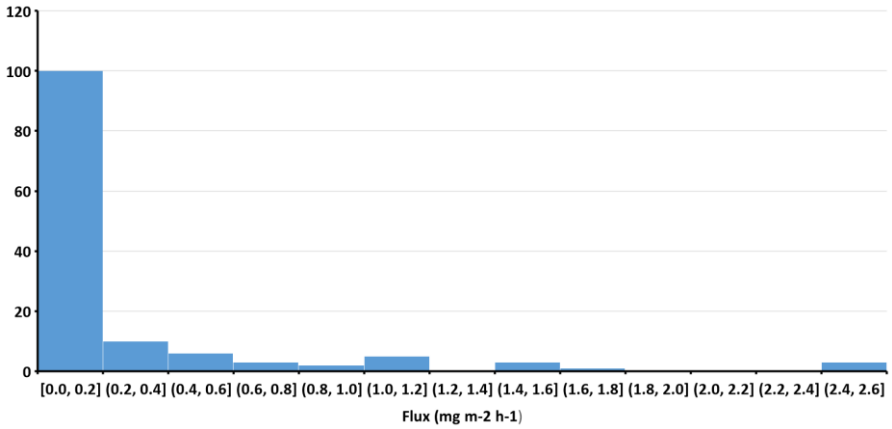

Figure 6. Histogram of N_2O fluxes measured using static chambers during the period 2019 – 2002 (n = 133 fluxes. Each flux is the average of 3 replicates)

Table 3. Annual emission in 2019, 2020, 2021, and 2022 and the average annual emission in 2019-2022 obtained by measurements using static chambers. The total emission is divided in the part due to relatively low "background emissions" (< 0.2 mg N_2O-N m^{-2} h^{r-1}) and the part due to peak emissions (≥ 0.2 mg N_2O-N m^{-2} h^{r-1}).

Year	Peak emission		Background emission		Total emission
	kg N_2O-N ha^{-1} yr^{-1}	%	kg N_2O-N ha^{-1} yr^{-1}	%	kg N_2O-N ha^{-1} yr^{-1}
2019	7.2	66	3.7	34	10.9
2020	13.0	78	3.6	22	16.6
2021	29.5	88	4.0	12	33.5
2022	7.3	70	3.1	30	10.5
Average	14.3	76	3.6	24	17.8

The Tier 1 IPCC default emission factor for N_2O from unfertilised drained peat soils is 8 kg N ha^{-1} yr^{-1} (with an uncertainty range of 2–24 kg N ha^{-1} yr^{-1} (Liang and Noble, 2019). The default emission factor for synthetic N fertiliser applied in wet climate is 1.6% of the N applied. On average 230 kg N ha^{-1} yr^{-1} was applied to grassland in the experiment, which means that the N_2O emission using the average Tier 1 approach of IPCC is 8 + 1.6% × 230 = 11.7 kg N ha^{-1} y^{-1}, which is somewhat smaller than the average annual N_2O emission of 17.8 kg N kg N ha^{-1} yr^{-1} in our study.

The annual emissions of 10 – 33 kg N kg N ha^{-1} yr^{-1} fall in the range of N_2O emissions obtained on the same dairy farm in Zegveld in other studies. Measurements of Velthof et al. (1996a) on other fields, showed emissions of 8.0 (drainage depth 40 cm) to 20.2 (drainage depth 55 cm) kg N ha^{-1} yr^{-1} for N fertilised (also using CAN) and mown grassland. Van Beek et al. (2011) reported annual N_2O emissions from fertilised and managed grasslands on the same dairy farm of 14 ± 3 kg N ha^{-1} yr^{-1} for fields with a drainage depth of 40 cm depth and 21 ± 2 kg N ha^{-1} yr^{-1} for fields with a drainage depth of 55 cm. Studies outside the Netherlands show similar or smaller N_2O emissions from grasslands on drained peat soils. Petersen et al. (2012) found that annual emissions from managed grasslands, both unfertilised and fertilised, on peat soils in Western Denmark ranged from about 3 to 9 kg N ha^{-1} yr^{-1}. Liu et al. (2020) estimated an average N_2O emission from grasslands on peat soils of 17.4 kg N ha^{-1} yr^{-1} in Europe. The annual N_2O emission from a deeply drained (drainage depth 0.7 m) managed grassland in Germany to which cattle slurry was applied was 3.9 ± 3.1 kg N ha^{-1} yr^{-1} (Offermanns et al., 2023).

The emission of N_2O was impacted by an interactive effect between the groundwater level and the availability of nitrate (NO_3^-) in the soil (LLR = 5.27; df = 1; *p*=0.023). Visualization of the regression of the main effects (NO_3^- and groundwater level) on N_2O emission is shown in Figure 6 of the Appendix. Other studies have shown that the content of NO_3^- and soil moisture content are main factors controlling N_2O emission from managed peat soils. In a laboratory study of Lohila et al. (2021), N_2O fluxes from the top layer of peat soils correlated positively with NO_3^- content at near water-saturated conditions. Velthof et al. (1996c) measured the spatial variability of N_2O fluxes from a managed grassland on peat soil. Fluxes were highest in the part of the field with highest NO_3^- contents, groundwater level and water-filled pore space.

Differences in N_2O fluxes were observed between 2021 and 2022 (Figure 8). This was most likely due to wetter conditions in 2021, with more precipitation throughout the summer and less decreases in groundwater level than in 2022 (Figure 8). In 2021, both N_2O fluxes and NO_3^- concentrations in the porewater were generally higher than in 2022 (Figure 8). Peaks in N_2O emission and, in the second half of the summer, NO_3^- availability, coincide with fertilisation events during wet periods (i.e., rainfall occurs immediately after fertiliser application). When fertiliser was applied during dry periods, such as September 2021 or April to September 2022, we observed no or only small N_2O peaks. In September 2021, fertilisation led to an increase in NO_3^- availability, but the N_2O flux did not increase. After rainfall in October, a delayed but large peak of N_2O emission was shown. In 2022, peaks in NO_3^- availability and N_2O emission occurred at the same time, after fertilisation events in April, July and September, with the latter event leading to the highest peaks.

In this experiment, CAN was used as N source, as it is the most used mineral N fertiliser in the Netherlands (about 60% of the total mineral N fertiliser uses in the Netherlands; Van Bruggen et al., 2022). The results show that directly adding NO_3^- with CAN during wet conditions increases the risk of N_2O emissions from peat soils, and that fertilisation events with CAN largely affect the temporal pattern of N_2O fluxes (Figures 5 and 8). It is known that N_2O emission is relatively high when CAN is applied under wet conditions to soils with high available C contents, such as grasslands and peat soils (Harty et al., 2016; Velthof et al., 1996a). In 2022, the experiment in Zegveld was expanded to include a treatment with cattle slurry. The N_2O emission from cattle slurry was smaller than that from CAN (data not shown). Dairy farms in the peat area in the Netherlands use both mineral N fertiliser and cattle slurry, which may suggest that the annual N_2O emissions from this experiment (Figure 5) are higher than those on the average dairy farms in the Dutch peat areas. However, the grassland in the experiment was mown only, whereas in practice, grasslands are both mown and grazed during the growing season. The N_2O emissions from grazed grassland on peat soils in Zegveld were a factor 2.1 to 2.6 higher than from mown grassland (Velthof et al., 1996a).

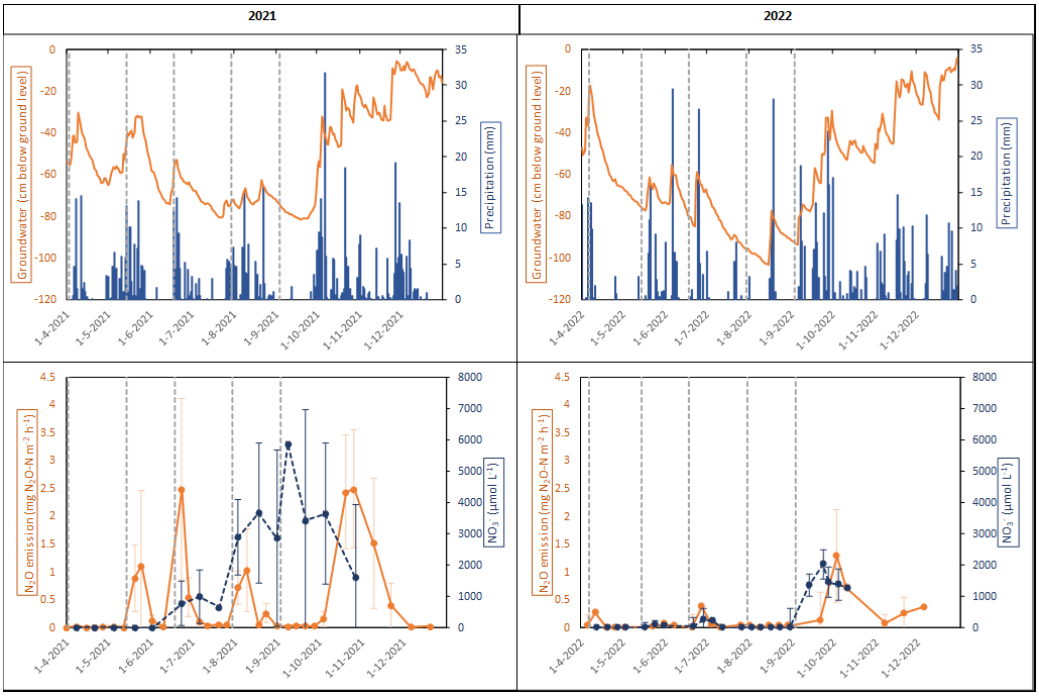

Figure 8. Upper figure: groundwater levels (relative to ground level) and precipitation (data from KNMI station Zegveld). Lower figure. Measurements of N_2O fluxes using static chamber (orange) and nitrate (NO_3^-) availability (blue) in the same control plot. All measurements were conducted between April and December 2021 (left) and 2022 (right). The fluxes are part of Vertical dotted lines indicate fertilisation events.

4 Synthesis and conclusions

The results automated chamber measurements during the period October 2022 – January 2023 showed that N_2O fluxes were low, but not negligible during winter (Figure 2). These measurements also showed that treatment of measurement data, such as filtering for turbulent atmospheric conditions, significantly affected the calculated N_2O flux at these low levels. This may be due to a methodological bias during nights with atmospheric stratification which so far has only been reported for CO_2 fluxes. This bias hampers an in-depth analysis of the factors controlling diurnal variations in N_2O fluxes during periods of low emission. A more in-depth analysis of data is needed to avoid that true diurnal variations related to stable atmosphere conditions are discarded using the filtering procedure.

Flux measurements with static chambers during 2019 – 2022 occasionally showed elevated fluxes outside the growing season (Figures 5 and 8). The period with relatively low emission contributed to only 24% of the total N_2O emission (Table 3). Velthof et al. (1996a) showed large differences in the contribution of non-growing season N_2O emission to total N_2O emission between two drained and N fertilised (CAN) peat soils. In a relatively wet peat soil (drainage depth: 40 cm) the N_2O emission in the period December - February contributed to 2.2 % of the total annual N_2O emission. The N_2O emission in the same period from the peat soil with more shallow groundwater level (drainage depth: 55 cm) contributed to 11% of the annual emission. In contrast, Pelster et al. (2022), showed for Canadian agricultural soils that N_2O emission continues at low rate during the non-growing season and that these emissions may account for a significant proportion (up to 35%) of annual emissions. This relatively high contribution of non-growing season N_2O emission in Canada is partly caused by high N_2O fluxes during freezing-thawing events (e.g., Wagner-Riddle et al., 2017). The climate in the winter in the Netherlands are mild compared to Canada, with generally no long periods of frost.

It is concluded from our paper that the temporal variation in N_2O emission from managed grasslands on peat soils is high at different time scales:

- Diurnal variations in N_2O emission are shown in periods with relatively low emissions (on average < 120 µg N m^{-2} h^{-1}), which are likely the result of a known and problematic methodological bias, resulting in spurious correlations of N_2O fluxes with other variables that vary diurnally, such as CO_2 fluxes and photosynthetically-active radiation;
- High N_2O emission peaks were shown directly after N application during wet conditions (heavy rainfall and high groundwater level). This peaks occurred at < 25% of measurement time during 4 year, but contributed to 76% of the total N_2O emission;
- Large annual variations in N_2O emission are shown (10.5 – 33.5 kg N ha^{-1} yr^{-1}), due to differences between years in the amount of rainfall in the period when nitrogen is applied.

Quantification of options to reduce N_2O emission requires a combination of measurement techniques, i.e. static chamber techniques with measurements at discrete intervals to compare mitigation options in a statistical sound experimental design in combination with automatic chambers and eddy co-variance techniques for insight in factors controlling N_2O emission, gap filling and extrapolation to a larger temporal and spatial scale. As large part of the annual N_2O emission is produced during relatively short events after N application and rainfall, measurement strategies should focus on an accurate quantification of these N_2O peaks.

5 Acknowledgements

This study was part of the Netherlands Research Programme on Greenhouse Gas Dynamics of Peatlands and Organic Soils (NOBV), which was launched in 2019 by the Dutch ministry of Agriculture, Nature management and Food quality (LNV) as part of the Climate Agreement. Its objective is to research the effectiveness of measures in peatland areas and to be able to better predict emission levels. The effect on subsidence is also researched. The programme is directed by the Foundation for Applied Water Research (STOWA). The research is conducted by Wageningen University (WU), Wageningen Environmental Research (WENR), Vrije Universiteit Amsterdam (VU), Utrecht University (UU), Radboud University, Deltares research institute.

6 References

Aben, R., Boonman, J., Van de Craats, D., Peeters, S., Van den Berg, M., Boonman, C., Van Giersbergen, Q., Heuts, T., Erkens, G., Van der Velde, Y., 2023. Effectiveness of subsoil irrigation techniques in reducing CO2 emission from drained peatlands, Dutch National Research Programme on Greenhouse Gases in Peatlands (NOBV).

Anthony, T.L., Silver, W.L., 2021. Hot moments drive extreme nitrous oxide and methane emissions from agricultural peatlands. Glob Chang Biol 27, 5141–5153. https://doi.org/10.1111/GCB.15802

Boonman, J., Hefting, M.M., Van Huissteden, C.J.A., Van Den Berg, M., Van Huissteden, J., Erkens, G., Melman, R., Van Der Velde, Y., 2022. Cutting peatland CO2 emissions with water management practices. Biogeosciences 19, 5707–5727. https://doi.org/10.5194/BG-19-5707-2022

Brændholt, A., Steenberg Larsen, K., Ibrom, A., Pilegaard, K., 2017. Overestimation of closed-chamber soil CO₂ effluxes at low atmospheric turbulence. Biogeosciences 14, 1603–1616. https://doi.org/10.5194/bg-14-1603-2017

Bruggen, C. van, Bannink, A., Bleeker, A., Bussink, D.W., Groenestein, C.M., Huijsmans, J.F.M., Kros, J., Lagerwerf, L.A., Luesink, H.H., Ros, M.B.H., Schijndel, M.W. van, Velthof, G.L., Zee, T. van der, 2022. Emissies naar lucht uit de landbouw berekend met NEMA voor 1990-2020. https://doi.org/10.18174/570194

Butterbach-Bahl, K., Baggs, E.M., Dannenmann, M., Kiese, R., Zechmeister-Boltenstern, S., 2013. Nitrous oxide emissions from soils: how well do we understand the processes and their controls? Philosophical Transactions of the Royal Society B: Biological Sciences 368. https://doi.org/10.1098/RSTB.2013.0122

Christiansen, J.R., Outhwaite, J., Smukler, S.M., 2015. Comparison of CO2, CH4 and N2O soil-atmosphere exchange measured in static chambers with cavity ring-down spectroscopy and gas chromatography. Agric For Meteorol C, 48–57. https://doi.org/10.1016/J.AGRFORMET.2015.06.004

de Klein, C.A.M., Alfaro, M.A., Giltrap, D., Topp, C.F.E., Simon, P.L., Noble, A.D.L., van der Weerden, T.J., 2020. Global Research Alliance N2O chamber methodology guidelines: Statistical considerations, emission factor calculation, and data reporting. J Environ Qual 49, 1156–1167. https://doi.org/https://doi.org/10.1002/jeq2.20127

Dickopp, J., Lengerer, A., Kazda, M., 2018. Relationship between groundwater levels and oxygen availability in fen peat soils. Ecol Eng 120, 85–93. https://doi.org/10.1016/J.ECOLENG.2018.05.033

Dorich, C., Fehr, B., Conant, R.T., 2019. Advanced statistical methods for gap-filling N2O emissions data. AGUFM 2019, B13L-2452.

Dorich, C.D., De Rosa, D., Barton, L., Grace, P., Rowlings, D., Migliorati, M.D.A., Wagner-Riddle, C., Key, C., Wang, D., Fehr, B., Conant, R.T., 2020. Global Research Alliance N2O chamber methodology guidelines: Guidelines for gap-filling missing measurements. J Environ Qual 49, 1186–1202. https://doi.org/https://doi.org/10.1002/jeq2.20138

Firestone, M.K., 1982. Biological Denitrification, in: Stevenson, F.J. (Ed.), Nitrogen in Agricultural Soils. Agron. Monogr. 22. American Society of Agronomy, Crop Science Society of America, and Soil Science Society of America, Madison, WI, pp. 289–326.

Fuss, R., 2020. Greenhouse Gas Flux Calculation from Chamber Measurements [R package gasfluxes version 0.4-4].

Goodrich, J.P., Wall, A.M., Campbell, D.I., Fletcher, D., Wecking, A.R., Schipper, L.A., 2021. Improved gap filling approach and uncertainty estimation for eddy covariance N2O fluxes. Agric For Meteorol 297. https://doi.org/10.1016/J.AGRFORMET.2020.108280

Görres, C.-M., Kammann, C., Ceulemans, R., 2016. Automation of soil flux chamber measurements: potentials and pitfalls. Biogeosciences 13, 1949–1966. https://doi.org/10.5194/bg-13-1949-2016

Harty, M.A., Forrestal, P.J., Watson, C.J., McGeough, K.L., Carolan, R., Elliot, C., Krol, D., Laughlin, R.J., Richards, K.G., Lanigan, G.J., 2016. Reducing nitrous oxide emissions by changing N fertiliser use from calcium ammonium nitrate (CAN) to urea based formulations. Science of The Total Environment 563–564, 576–586. https://doi.org/https://doi.org/10.1016/j.scitotenv.2016.04.120

Hüppi, R., Felber, R., Krauss, M., Six, J., Leifeld, J., Fuß, R., 2018. Restricting the nonlinearity parameter in soil greenhouse gas flux calculation for more reliable flux estimates. PLoS One 13, e0200876. https://doi.org/10.1371/JOURNAL.PONE.0200876

Hutchinson, G.L., Mosier, A.R., 1981. Improved Soil Cover Method for Field Measurement of Nitrous Oxide Fluxes. Soil Science Society of America Journal 45, 311–316. https://doi.org/10.2136/sssaj1981.03615995004500020017x

IPCC, 2014. Supplement to the 2006 IPCC Guidelines for National greenhouse gas inventories. Wetlands., in: IPCC Guidelines for National Greenhouse Gas Inventories.

Juszczak, R., Acosta, M., Olejnik, J., 2012. Comparison of Daytime and Nighttime Ecosystem Respiration Measured by the Closed Chamber Technique on a Temperate Mire in Poland. Pol J Environ Stud 21, 643–658.

Keane, B.J., Ineson, P., Vallack, H.W., Blei, E., Bentley, M., Howarth, S., McNamara, N.P., Rowe, R.L., Williams, M., Toet, S., 2018a. Greenhouse gas emissions from the energy crop oilseed rape (Brassica napus); the role of photosynthetically active radiation in diurnal N2O flux variation. GCB Bioenergy 10, 306–319. https://doi.org/https://doi.org/10.1111/gcbb.12491

Keane, B.J., Ineson, P., Vallack, H.W., Blei, E., Bentley, M., Howarth, S., McNamara, N.P., Rowe, R.L., Williams, M., Toet, S., 2018b. Greenhouse gas emissions from the energy crop oilseed rape (Brassica napus); the role of photosynthetically active radiation in diurnal N2O flux variation. GCB Bioenergy 10, 306–319. https://doi.org/https://doi.org/10.1111/gcbb.12491

Koskinen, M., Minkkinen, K., Ojanen, P., Kämäräinen, M., Laurila, T., Lohila, A., 2014. Measurements of CO2 exchange with an automated chamber system throughout the year: challenges in measuring night-time respiration on porous peat soil. Biogeosciences 11, 347–363. https://doi.org/10.5194/bg-11-347-2014

Kroon, P.S., Schrier-Uijl, A.P., Hensen, A., Veenendaal, E.M., Jonker, H.J.J., 2010. Annual balances of CH4 and N2O from a managed fen meadow using eddy covariance flux measurements. Eur J Soil Sci 61, 773–784. https://doi.org/10.1111/J.1365-2389.2010.01273.X

Lai, D.Y.F., Roulet, N.T., Humphreys, E.R., Moore, T.R., Dalva, M., 2012. The effect of atmospheric turbulence and chamber deployment period on autochamber CO2 and CH4 flux measurements in an ombrotrophic peatland. Biogeosciences 9, 3305–3322. https://doi.org/10.5194/BG-9-3305-2012

Leppelt, T., Dechow, R., Gebbert, S., Freibauer, A., Lohila, A., Augustin, J., Drösler, M., Fiedler, S., Glatzel, S., Höper, H., Järveoja, J., Lærke, P.E., Maljanen, M., Mander, Mäkiranta, P., Minkkinen, K., Ojanen, P., Regina, K., Strömgren, M., 2014. Nitrous oxide emission budgets and land-use-driven hotspots for organic soils in Europe. Biogeosciences 11, 6595–6612. https://doi.org/10.5194/BG-11-6595-2014

Liang, C., Noble, A., 2019. Chapter 11: N2O Emissions from Managed Soils, and CO2 Emissions from Lime and Urea Application Chapter 11 N2O emissions from managed soils, and CO2 emissions from lime and urea application.

Liu, H., Wrage-Mönnig, N., Lennartz, B., 2020. Rewetting strategies to reduce nitrous oxide emissions from European peatlands. Commun Earth Environ 1. https://doi.org/10.1038/S43247-020-00017-2

Lohila, A., Li, Y., Glatzel, S., Norberg, L., Hellman, M., Berglund, K., Hallin, S., Berglund, Ö., 2021. Methane and Nitrous Oxide Production From Agricultural Peat Soils in Relation to Drainage Level and Abiotic and Biotic Factors. https://doi.org/10.3389/fenvs.2021.631112

Maag, M., Vinther, F.P., 1996. Nitrous oxide emission by nitrification and denitrification in different soil types and at different soil moisture contents and temperatures. Applied Soil Ecology 4, 5–14. https://doi.org/10.1016/0929-1393(96)00106-0

Maier, M., Weber, T.K.D., Fiedler, J., Fuß, R., Glatzel, S., Huth, V., Jordan, S., Jurasinski, G., Kutzbach, L., Schäfer, K., Weymann, D., Hagemann, U., 2022. Introduction of a guideline for measurements of greenhouse gas fluxes from soils using non-steady-state chambers. Journal of Plant Nutrition and Soil Science 185, 447–461. https://doi.org/https://doi.org/10.1002/jpln.202200199

Maljanen, M., Martikainen, P.J., Aaltonen, H., Silvola, J., 2002. Short-term variation in fluxes of carbon dioxide, nitrous oxide and methane in cultivated and forested organic boreal soils. Soil Biol Biochem 34, 577–584. https://doi.org/10.1016/S0038-0717(01)00213-9

Munch, J.C., Velthof, G.L., 2007. Denitrification and Agriculture. Biology of the Nitrogen Cycle 331–341. https://doi.org/10.1016/B978-044452857-5.50022-9

Nickerson, N., 2016. Evaluating gas emission measurements using Minimum Detectable Flux (MDF).

Offermanns, L., Tiemeyer, B., Dettmann, U., Rüffer, J., Düvel, D., Vogel, I., Brümmer, C., 2023. High greenhouse gas emissions after grassland renewal on bog peat soil. Agric For Meteorol 331, 109309. https://doi.org/10.1016/j.agrformet.2023.109309

Pastorello, G., Trotta, C., Canfora, E., Chu, H., Christianson, D., Cheah, Y.W., Poindexter, C., Chen, J., Elbashandy, A., Humphrey, M., Isaac, P., Polidori, D., Ribeca, A., van Ingen, C., Zhang, L., Amiro, B., Ammann, C., Arain, M.A., Ardö, J., Arkebauer, T., Arndt, S.K., Arriga, N., Aubinet, M., Aurela, M., Baldocchi, D., Barr, A., Beamesderfer, E., Marchesini, L.B., Bergeron, O., Beringer, J., Bernhofer, C., Berveiller, D., Billesbach, D., Black, T.A., Blanken, P.D., Bohrer, G., Boike, J., Bolstad, P. V., Bonal, D., Bonnefond, J.M., Bowling, D.R., Bracho, R., Brodeur, J., Brümmer, C., Buchmann, N., Burban, B., Burns, S.P., Buysse, P., Cale, P., Cavagna, M., Cellier, P., Chen, S., Chini, I., Christensen, T.R., Cleverly, J., Collalti, A., Consalvo, C., Cook, B.D., Cook, D., Coursolle, C., Cremonese, E., Curtis, P.S., D'Andrea, E., da Rocha, H., Dai, X., Davis, K.J., De Cinti, B., de Grandcourt, A., De Ligne, A., De Oliveira, R.C., Delpierre, N., Desai, A.R., Di Bella, C.M., di Tommasi, P., Dolman, H., Domingo, F., Dong, G., Dore, S., Duce, P., Dufrêne, E., Dunn, A., Dušek, J., Eamus, D., Eichelmann, U., ElKhidir, H.A.M., Eugster, W., Ewenz, C.M., Ewers, B., Famulari, D., Fares, S., Feigenwinter, I., Feitz, A., Fensholt, R., Filippa, G., Fischer, M., Frank, J., Galvagno, M., Gharun, M., Gianelle, D., Gielen, B., Gioli, B., Gitelson, A., Goded, I., Goeckede, M., Goldstein, A.H., Gough, C.M., Goulden, M.L., Graf, A., Griebel, A., Gruening, C., Grünwald, T., Hammerle, A., Han, S., Han, X., Hansen, B.U., Hanson, C., Hatakka, J., He, Y., Hehn, M., Heinesch, B., Hinko-Najera, N., Hörtnagl, L., Hutley, L., Ibrom, A., Ikawa, H., Jackowicz-Korczynski, M., Janouš, D., Jans, W., Jassal, R., Jiang, S., Kato, T., Khomik, M., Klatt, J., Knohl, A., Knox, S., Kobayashi, H., Koerber, G., Kolle, O., Kosugi, Y., Kotani, A., Kowalski, A., Kruijt, B., Kurbatova, J., Kutsch, W.L., Kwon, H., Launiainen, S., Laurila, T., Law, B., Leuning, R., Li, Yingnian, Liddell, M., Limousin, J.M., Lion, M., Liska, A.J., Lohila, A., López-Ballesteros, A., López-Blanco, E., Loubet, B., Loustau, D., Lucas-Moffat, A., Lüers, J., Ma, S., Macfarlane, C., Magliulo, V., Maier, R., Mammarella, I., Manca, G., Marcolla, B., Margolis, H.A., Marras, S., Massman, W., Mastepanov, M., Matamala, R., Matthes, J.H., Mazzenga, F., McCaughey, H., McHugh, I., McMillan, A.M.S., Merbold, L., Meyer, W., Meyers, T., Miller, S.D., Minerbi, S., Moderow, U., Monson, R.K., Montagnani, L., Moore, C.E., Moors, E., Moreaux, V., Moureaux, C., Munger, J.W., Nakai, T., Neirynck, J., Nesic, Z., Nicolini, G., Noormets, A., Northwood, M., Nosetto, M., Nouvellon, Y., Novick, K., Oechel, W., Olesen, J.E., Ourcival, J.M., Papuga, S.A., Parmentier, F.J., Paul-Limoges, E., Pavelka, M., Peichl, M., Pendall, E., Phillips, R.P., Pilegaard, K., Pirk, N., Posse, G., Powell, T., Prasse, H., Prober, S.M., Rambal, S., Rannik, Ü., Raz-Yaseef, N., Reed, D., de Dios, V.R., Restrepo-Coupe, N., Reverter, B.R., Roland, M., Sabbatini, S., Sachs, T., Saleska, S.R., Sánchez-Cañete, E.P., Sanchez-Mejia, Z.M., Schmid, H.P., Schmidt, M., Schneider, K., Schrader, F., Schroder, I., Scott, R.L., Sedlák, P., Serrano-Ortíz, P., Shao, C., Shi, P., Shironya, I., Siebicke, L., Šigut, L., Silberstein, R., Sirca, C., Spano, D., Steinbrecher, R.,

Stevens, R.M., Sturtevant, C., Suyker, A., Tagesson, T., Takanashi, S., Tang, Y., Tapper, N., Thom, J., Tiedemann, F., Tomassucci, M., Tuovinen, J.P., Urbanski, S., Valentini, R., van der Molen, M., van Gorsel, E., van Huissteden, K., Varlagin, A., Verfaillie, J., Vesala, T., Vincke, C., Vitale, D., Vygodskaya, N., Walker, J.P., Walter-Shea, E., Wang, H., Weber, R., Westermann, S., Wille, C., Wofsy, S., Wohlfahrt, G., Wolf, S., Woodgate, W., Li, Yuelin, Zampedri, R., Zhang, J., Zhou, G., Zona, D., Agarwal, D., Biraud, S., Torn, M., Papale, D., 2020. The FLUXNET2015 dataset and the ONEFlux processing pipeline for eddy covariance data. Scientific Data 2020 7:1 7, 1–27. https://doi.org/10.1038/S41597-020-0534-3

Petersen, S.O., Hoffmann, C.C., Schäfer, C.-M., Blicher-Mathiesen, G., Elsgaard, L., Kristensen, K., Larsen, S.E., Torp, S.B., Greve, M.H., 2012. Annual emissions of CH 4 and N 2 O, and ecosystem respiration, from eight organic soils in Western Denmark managed by agriculture. Biogeosciences 9, 403–422. https://doi.org/10.5194/bg-9-403-2012

Rochette, P., Hutchinson, G.L., 2005. Measurement of Soil Respiration in situ: Chamber Techniques, in: Micrometeorology in Agricultural Systems, Agronomy Monographs. pp. 247–286. https://doi.org/https://doi.org/10.2134/agronmonogr47.c12

Säurich, A., Tiemeyer, B., Dettmann, U., Don, A., 2019. How do sand addition, soil moisture and nutrient status influence greenhouse gas fluxes from drained organic soils? Soil Biol Biochem 135, 71–84. https://doi.org/10.1016/J.SOILBIO.2019.04.013

Schneider, J., Kutzbach, L., Schulz, S., Wilmking, M., 2009. Overestimation of CO2 respiration fluxes by the closed chamber method in low-turbulence nighttime conditions. J Geophys Res Biogeosci 114. https://doi.org/https://doi.org/10.1029/2008JG000909

Smith, K.A., Dobbie, K., 2001. The impact of sampling frequency and sampling times on chamber-based measurements of N2O emissions from fertilized soils. Glob Chang Biol 7, 933–945. https://doi.org/10.1046/J.1354-1013.2001.00450.X

Taft, H.;, Cross, P.;, Jones, D.L., 2018. Efficacy of mitigation measures for reducing greenhouse gas emissions from intensively cultivated peatlands. Soil Biol Biochem. https://doi.org/10.1016/j.soilbio.2018.08.020

van Beek, C.L., Pleijter, M., Kuikman, P.J., 2011. Nitrous oxide emissions from fertilized and unfertilized grasslands on peat soil. Nutr Cycl Agroecosyst 89, 453–461. https://doi.org/10.1007/S10705-010-9408-Y/FIGURES/4

Velthof, G.L., Brader, A.B., Oenema, O., 1996a. Seasonal variations in nitrous oxide losses from managed grasslands in The Netherlands. Plant Soil 181, 263–274. https://doi.org/10.1007/BF00012061

Velthof, G.L., Koops, J.G., Duyzer, J.H., Oenema, O., 1996b. Prediction of nitrous oxide fluxes from managed grassland on peat soil using a simple empirical model. Netherlands Journal of Agricultural Science 44, 339–356. https://doi.org/10.18174/NJAS.V44I4.541

Wagner-Riddle, C., Congreves, K.A., Abalos, D., Berg, A.A., Brown, S.E., Ambadan, J.T., Gao, X., Tenuta, M., 2017. Globally important nitrous oxide emissions from croplands induced by freeze-thaw cycles. https://doi.org/10.1038/NGEO2907

Wecking, A.R., Wall, A.M., Liáng, L.L., Lindsey, S.B., Luo, J., Campbell, D.I., Schipper, L.A., 2020. Reconciling annual nitrous oxide emissions of an intensively grazed dairy pasture determined by eddy covariance and emission factors. Agric Ecosyst Environ 287, 106646. https://doi.org/10.1016/J.AGEE.2019.106646

Weier, K.L., Doran, J.W., Power, J.F., Walters, D.T., 1993. Denitrification and the Dinitrogen/Nitrous Oxide Ratio as Affected by Soil Water, Available Carbon, and Nitrate. Soil Science Society of America Journal 57, 66–72. https://doi.org/https://doi.org/10.2136/sssaj1993.03615995005700010013x

Wrage-Mönnig, N., Horn, M.A., Well, R., Müller, C., Velthof, G., Oenema, O., 2018. The role of nitrifier denitrification in the production of nitrous oxide revisited. Soil Biol Biochem 123, A3–A16. https://doi.org/10.1016/J.SOILBIO.2018.03.020

Zhu, S., McCalmont, J., Cardenas, L.M., Cunliffe, A.M., Olde, L., Signori-Müller, C., Litvak, M.E., Hill, T., 2023. Gap-filling carbon dioxide, water, energy, and methane fluxes in challenging ecosystems: comparing between methods, drivers, and gap-lengths. Agric For Meteorol 332, 109365. https://doi.org/10.1016/J.AGRFORMET.2023.109365

7 Appendix

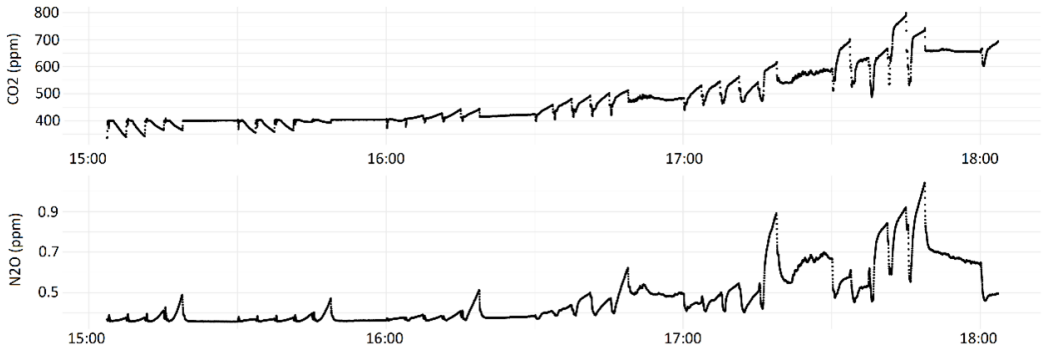

Figure A1. *Examples of pulse emissions of CO_2 and N_2O occurring immediately after chamber closure during establishment of atmospheric stabilisation.*

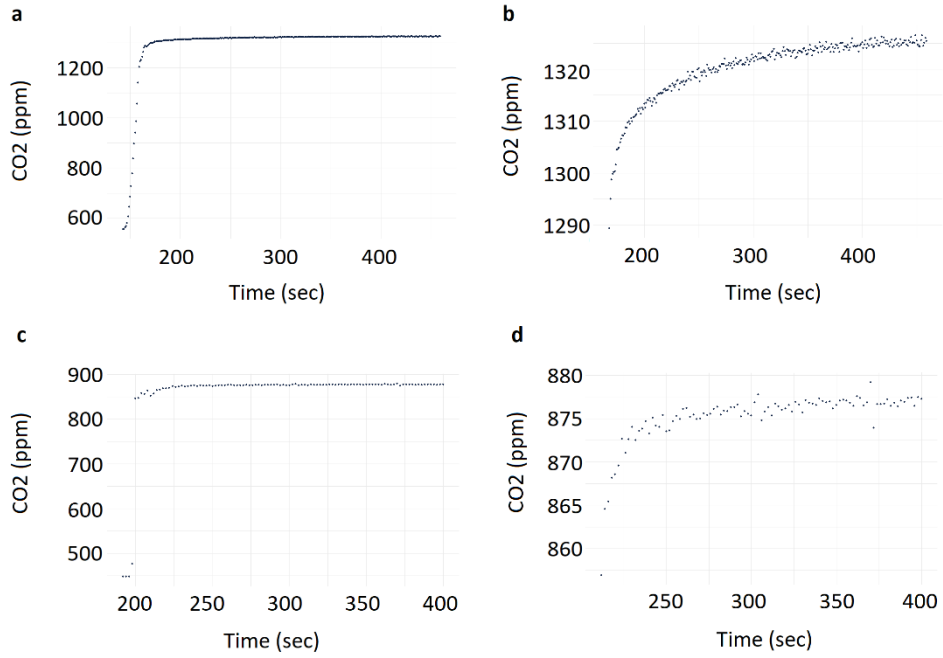

Figure A2. *Examples of mixing times after injecting a CO_2 pulse in a closed eosAC-LT chamber on an impermeable base. Figures a and b (zoomed in after initial peak) represent the result of a ~770 ppm CO_2 increase. Figures c and d (zoomed in after initial peak) represent the result of a ~430 ppm CO_2 increase.*

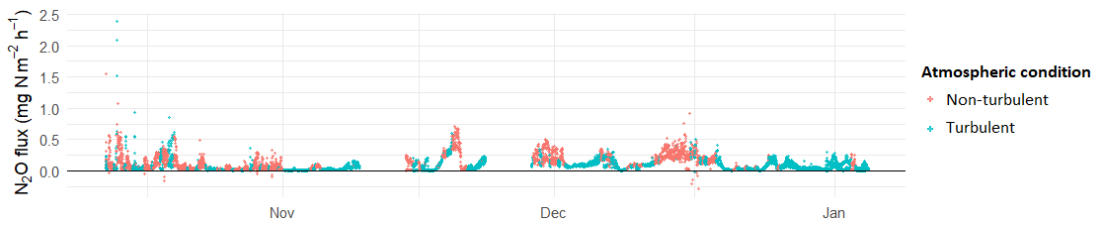

Figure A3. *Visualisation of chamber measurements that were classified as measured under turbulent (green dots; CO_2 concentration at start of measurement <= 420 ppm; 5205 measurements) and non-turbulent (red dots; CO_2 concentration at start of measurement > 420 ppm; 3312 measurements) atmospheric conditions.*

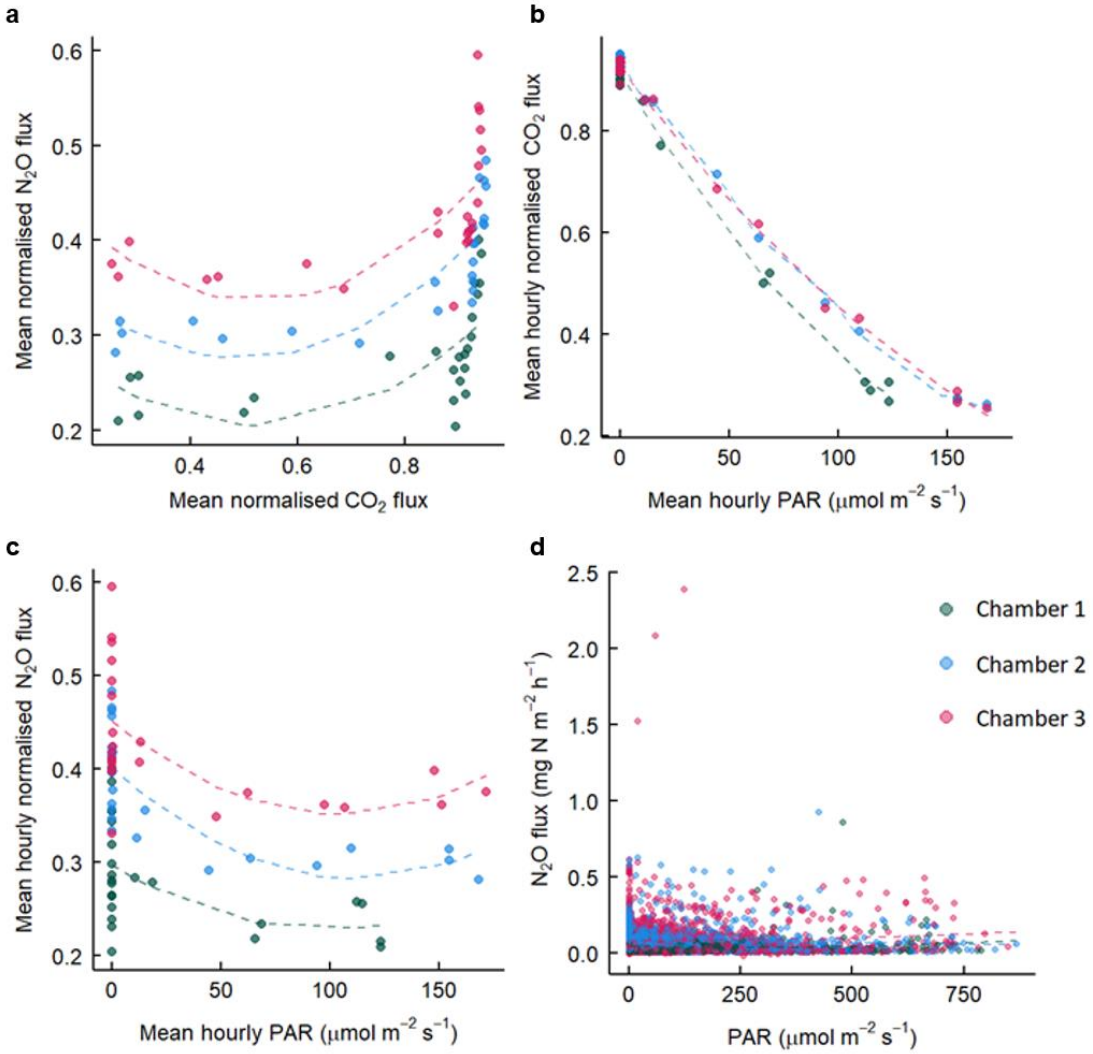

Fig. A4. *Plots of the normalised N_2O flux against the mean normalised CO_2 flux (a), mean hourly photosynthetically-active radiation (PAR) against the mean hourly normalised CO_2 flux (b), mean hourly PAR against the mean hourly normalised N_2O flux (c), and (d) PAR against the N_2O flux. Normalisation of data was achieved per chamber and day by min–max scaling (0–1) and subsequent binning by hour of day. Data are filtered by CO_2 concentrations <= 420 ppm at the start of chamber closure to largely exclude measurements in stable atmosphere.*

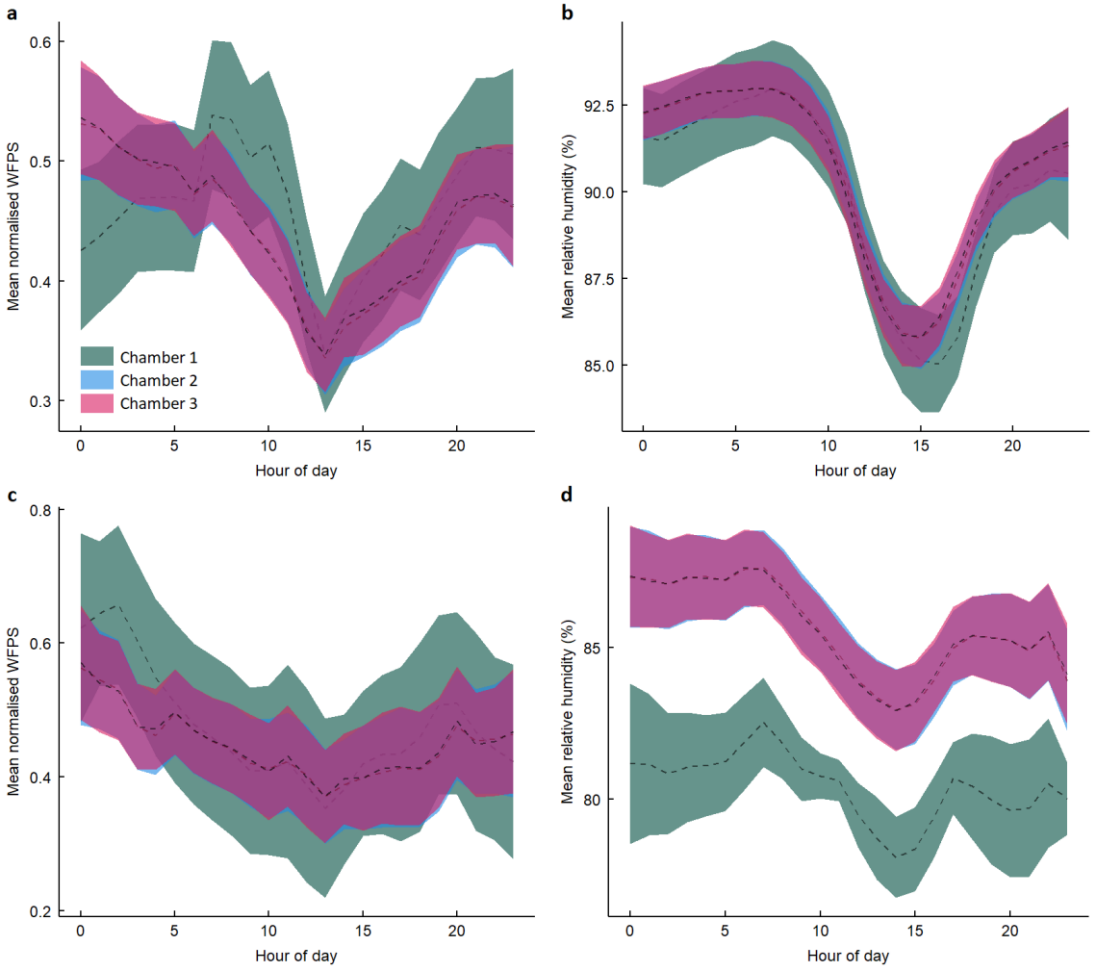

Figure A5. *Diurnal variation of mean normalised water-filled pore space (WFPS; estimated from soil moisture data via calibration with tensiometers) at 5 cm depth (a) and mean relative humidity at 150 cm height (b) during chamber measurements for the full study period and full dataset, and diurnal variation of mean normalised WFPS at 5 cm depth (c) and relative humidity at 150 cm height (d) during chamber measurements for the full study period filtered by CO_2 concentrations <= 420 ppm at the start of chamber closure to largely exclude measurements in stable atmosphere. WFPS during chamber measurements was normalised per chamber and day by min–max scaling (0–1). Relative humidity and normalised WFPS data were subsequently binned by hour of day. Dashed lines represent mean hourly values for each chamber. Shaded areas represent the standard error about the mean hourly values.*

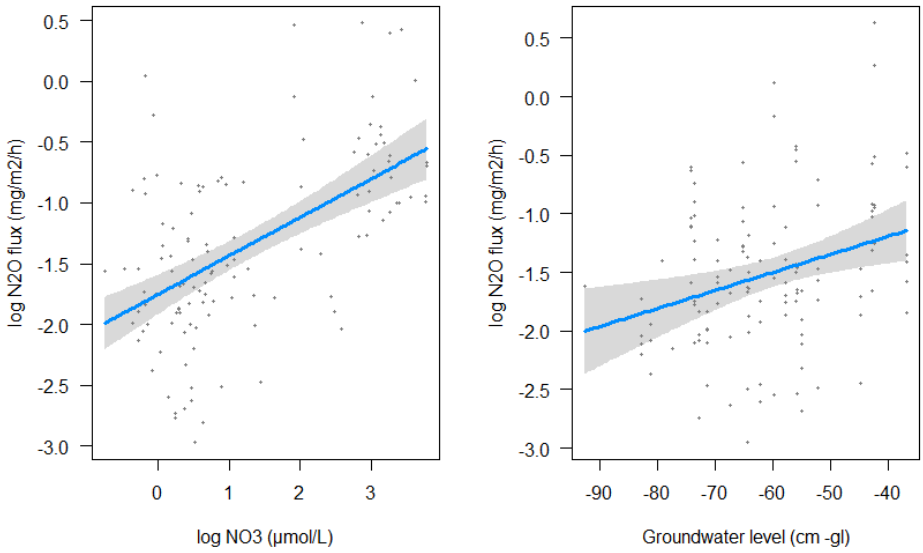

Figure A6. *Visualisation of Regression Models using Visreg of R of the plotted main effects of NO_3 (log(10)NO3; left) and Groundwater levels (right) against N_2O emission (log10N2O).*